A theoretical study of the zero-temperature Knight shifts in the high-T_c compound $YBa_2Cu_3O_7$

1992 J. Phys.: Condens. Matter 4 6253

(http://iopscience.iop.org/0953-8984/4/29/009)

J. Phys.: Condens. Matter 4 (1992) 6253–6266. Printed in the UK

A theoretical study of the zero-temperature Knight shifts in the high-T_c compound $YBa_2Cu_3O_7$

W Götz and H Winter

Kernforschungszentrum Karlsruhe, Institut für Nukleare Festkörperphysik, PO Box 3640, W-7500 Karlsruhe, Federal Republic of Germany

Received 14 February 1992

Abstract. Using the data from LSDFA LMTO ASA band-structure calculations we evaluate the zero-temperature Knight shifts K at the individual atoms of the stoichiometric high-T_c material $YBa_2Cu_3O_7$. All contributions to K are calculated—without using adjustable parameters—on the level of the previously described RPA-like spin-density-functional formalism approach. As a whole the results for the Cu atoms turn out to be in reasonably good agreement with experiment.

1. Introduction

Because of their spectacular superconducting properties, ceramic materials have attracted a great deal of attention during the last few years. Whereas the parent compound La_2CuO_4 causes extra difficulties in a theoretical treatment, since it becomes superconducting only on doping, $YBa_2Cu_3O_7$ is an example of a stoichiometric high-T_c material and is thus accessible to a description making use of Bloch symmetry without invoking approximations inherent for example in a KKR CPA kind of alloy theory.

There is some controversy as to how to treat the electronic structure of these kinds of system. This mainly dates back to investigations of the pure compound La_2CuO_4. Spin-polarized local-density-functional band-structure calculations failed badly to reproduce the experimentally established isolating antiferromagnetic ground state of this system. In contrast, they yielded a metallic state caused by a broad, strongly Cu $d_{x^2-y^2}$–planar O p_x, p_y-hybridized band crossing the Fermi surface (see, e.g., Matheiss (1987) and Temmerman *et al* (1988)). Moreover, as calculations of the spin susceptibility have shown (Leung *et al* 1988, Winter *et al* 1990), the local-spin-density-functional approximation (LSDFA) puts this system far from any magnetic instability for the wavevector q at the X point. Observations of this kind led many investigators to the decision to abstain from attempting to describe the ceramic materials by the LSDFA band-structure theory at all, but to apply instead some t–J or Hubbard model, devised for coping with strongly correlated electrons (see, e.g., Hirch and Marsiglio (1989) and Emery (1991)). Various spectroscopic experiments and the measurement of transport coefficients, however, reveal that, on doping, La_2CuO_4 readily becomes a metal. Unfortunately, most quantitative theoretical investigations on this transition encounter complications when dealing with a non-stoichiometric system.

0953-8984/92/296253+14$04.50

In this respect the situation is much simpler in the case of $YBa_2Cu_3O_7$. In qualitative accordance with experiment, LSDFA band-structure calculations yield a metallic ground state for this stoichiometric system and de Haas–van Alphen experiments show that a Fermi surface exists (Olsen *et al* 1990). The question arises of how good the quantitative agreement between LSDFA band-structure theories and measurements is. As pointed out in the comprehensive review article by Pickett (1989), charge densities are surprisingly well reproduced. The same is true for charge-density-related quantities such as phonon frequencies and electric-field gradients (Schwarz *et al* 1990). This statement even holds for the evaluation of such quantities in pure La_2CuO_4 (Cohen *et al* 1988). Apart from the bad failure of the LSDFA for La_2CuO_4 and $YBa_2Cu_3O_6$, magnetic properties are thought to be less well accounted for in metallic ceramic systems as well.

To shed some light on this controversy we set out to investigate the magnetic properties of $YBa_2Cu_3O_7$ using the band-structure-based parameter-free SDFA RPA method to evaluate magnetic correlation functions (Stenzel and Winter 1985, 1986, Stenzel *et al* 1988, Götz and Winter 1989, 1991). As a first step, we treat the zero-temperature Knight shifts of the individual atoms in this paper, which is organized as follows. In section 2 we give an outline of the formalism and display the LMTO-ASA band-structure results in section 3. Section 4 shows our theoretical results and section 5 compares them with experiment. In section 6 we contrast our method to semiempirical phenomenological treatments available in the literature. We close with some conclusions in section 7.

2. Formalism

A formulation of the contributions to K for cubic systems with one atom per unit cell in the rigorous language of correlation functions has already been given elsewhere (Götz and Winter (1991) and references therein). In the present case we deal with a non-cubic multicomponent compound, allowing us to study the anisotropy effects and to evaluate K at the individual atoms. Moreover, some researchers use model Hamiltonians and employ a somewhat doubtful terminology concerning the decomposition of K into various contributions and connecting them with susceptibilities. It might therefore be worthwhile to give a short sketch of the formalism in this work as well.

We start with the following non-relativistic hyperfine Hamiltonian as for example given by Bloembergen and Rowland (1953):

$$H_{\mathrm{hf}} = \int \mathrm{d}r\, \frac{16\pi}{3}\mu_{\mathrm{B}}\gamma_{\mathrm{n}}\hbar \boldsymbol{I}\cdot\boldsymbol{S}(\boldsymbol{r})\delta(\boldsymbol{r}) - 2\mu_{\mathrm{B}}\gamma_{\mathrm{n}}\hbar\boldsymbol{I}\cdot\left(\frac{\boldsymbol{S}(\boldsymbol{r})}{r^3} - \frac{3\boldsymbol{r}[\boldsymbol{r}\cdot\boldsymbol{S}(\boldsymbol{r})]}{r^5}\right) - (\gamma_{\mathrm{n}}\hbar e/mc)\left(\boldsymbol{I}\times\boldsymbol{r}/r^3\right)\cdot\boldsymbol{j}(\boldsymbol{r}). \tag{2.1}$$

Here, $\boldsymbol{I}$ is the nuclear spin located at the origin, $\boldsymbol{S}$ is the spin-density and $\boldsymbol{j}$ is the current density of the electrons. The relation between $\boldsymbol{j}$ on the one hand and the momentum density $\boldsymbol{p}$ of the electrons and an external vector potential $\boldsymbol{A}$ on the other hand is

$$\boldsymbol{j}(\boldsymbol{r}) = \boldsymbol{p}(\boldsymbol{r}) - (e/c)n(\boldsymbol{r})\boldsymbol{A}. \tag{2.2}$$

A static external magnetic field $\boldsymbol{H}$ of the form $\boldsymbol{H}_0 \exp(\mathrm{i}\boldsymbol{q}\cdot\boldsymbol{r})$ perturbs the electrons according to the relation

$$\delta H = \int \mathrm{d}r\, \boldsymbol{S}(r)\cdot\boldsymbol{H}(r) - \frac{e}{mc}\frac{1}{\mathrm{i}}\int \mathrm{d}r\, \boldsymbol{A}(r)\cdot\boldsymbol{p}(r). \tag{2.3}$$

The vector potential $\boldsymbol{A}$ is related to $\boldsymbol{H}$ by the formula $\boldsymbol{H} = \nabla \times \boldsymbol{A}$ and, choosing the Coulomb gauge ($\nabla\cdot\boldsymbol{A} = 0$), is given by

$$\boldsymbol{A}(r) = (1/\mathrm{i})[(\boldsymbol{q}\times\boldsymbol{H}_0)/q^2]\exp(\mathrm{i}\boldsymbol{q}\cdot\boldsymbol{r}). \tag{2.4}$$

The expectation value of H_{hf} in the linear approximation with respect to the perturbation (2.3) is proportional to K and it is straightforward to express the individual contributions in terms of the lattice transforms χ_q of correlation functions. We obtain

$$K = (1/\mu_{\mathrm{B}}\gamma_{\mathrm{n}}\hbar)\langle H_{\mathrm{hf}}\rangle = K_{\mathrm{s,c}} + K_{\mathrm{s,dip}} + K_{\mathrm{orb,para}} + K_{\mathrm{orb,dia}}. \tag{2.5}$$

In equation (2.5) we decompose K into the spin-contact part $K_{\mathrm{s,c}}$, the spin-dipole part $K_{\mathrm{s,dip}}$, the paramagnetic orbital part $K_{\mathrm{orb,para}}$ and the diamagnetic orbital part $K_{\mathrm{orb,dia}}$. They are defined by the following relations:

$$K_{\mathrm{s,c}}^{(\kappa,\beta)} = \lim_{q\to 0}\sum_{\alpha,\kappa'}\frac{16\pi}{3}\int \mathrm{d}\rho'\, I_{\alpha\kappa}\chi_q^{s\,\alpha,\beta}(0\kappa,\rho'\kappa';0)$$

$$K_{\mathrm{s,dip}}^{(\kappa,\beta)} = \lim_{q\to 0} -\sum_{\alpha,\overline{\alpha},\kappa'} I_{\alpha\kappa}\int \mathrm{d}\rho\,\mathrm{d}\rho'\left(\frac{\delta_{\alpha\overline{\alpha}}}{\rho^3} - \frac{3\rho_\alpha\rho_{\overline{\alpha}}}{\rho^5}\right)\chi_q^{s\,\overline{\alpha},\beta}(\rho\kappa,\rho'\kappa';0)$$

$$K_{\mathrm{orb,para}}^{(\kappa,\beta)} = -\sum_{\substack{\alpha,\gamma\\ \delta,\kappa'}}\lim_{q\to 0}\int \mathrm{d}\rho\,\mathrm{d}\rho'\, I_{\alpha\kappa}\epsilon_{\alpha\gamma\delta}\frac{\rho_\gamma}{\rho^3}\chi_q^{\mathrm{mom}\,\delta,\beta}(\rho\kappa,\rho'\kappa';0)\frac{1}{H_0} \tag{2.6}$$

$$\times\,(|\boldsymbol{q}\times\boldsymbol{H}|/q^2)_\beta\exp(\mathrm{i}\boldsymbol{q}\cdot\boldsymbol{\rho}')$$

$$K_{\mathrm{orb,dia}}^{(\kappa,\beta)} = -\frac{2}{\pi}\lim_{q\to 0}\int \mathrm{d}\epsilon\, f(\epsilon)\int\frac{\mathrm{d}k}{\Omega_{BZ}}\int \mathrm{d}\rho\, I_\kappa\cdot\frac{|\rho\times(q\times e_\beta)|}{q^2}$$

$$\times\exp(\mathrm{i}q\rho)\,\mathrm{Im}[g_k(\rho\kappa,\rho\kappa;\epsilon)].$$

In equations (2.6) we used local coordinates defined by $r = \rho + \tau_\kappa + R_j$ and performed the lattice transformations with respect to the cell coordinates R_j. The superscripts (κ,β) designate the site and the direction of the magnetic field, the sums over κ' run over the atoms of one unit cell and the integrals over ρ' and ρ, respectively, cover the Wigner–Seitz cells of the corresponding sites. The Greek indices stand for Cartesian components and g_k is the lattice transform of the one-particle Green function. To evaluate K we thus need the long-wavelength spin-density correlation function χ^{s} and momentum-density correlation function χ^{mom} for $\omega = 0$ (the last argument of the χ). For more detail we refer the reader to the papers of Stenzel and Winter (1985, 1986). Unlike Mila and Rice (1989a, b) who introduced the tensor **A** to mediate the nuclear momentum–electron spin coupling, our formulation is parameter-free, defining **A** on a microscopic level. Because of the spin-dipole term (Carter *et al* 1977) that does not vanish in the tetragonal structure considered in this

work, **A** is anisotropic. Moreover $K_{\mathrm{orb,para}}$ turns out to depend significantly on the direction β of the external magnetic field. Our formulation takes account of both on-site and site-off-diagonal (transferred hyperfine field) contributions, since we work with lattice transforms and sum over the sites κ'.

Our way of calculating χ_q^s in the LSDFA RPA approximation has been previously described (Stenzel and Winter 1986, Winter *et al* 1990). Here we quote only the integral equation which has to be set up and solved for χ^s. It reads (for the components α, α)

$$\chi_q^s(\rho\kappa, \rho'\kappa'; \omega) = \chi_q^{sP}(\rho\kappa, \rho'\kappa'; \omega) + \sum_{\kappa_1} \int \mathrm{d}\rho_1 \, \chi_q^{sP}(\rho\kappa, \rho_1\kappa_1; \omega) \times K_{xc}^s(\rho_1\kappa_1)\chi_q^s(\rho_1\kappa_1, \rho'\kappa'; \omega). \tag{2.7}$$

The non-interacting susceptibility χ_q^{sP} and the kernel K_{xc}^s can be expressed by the Bloch states $\psi_{k,\lambda}$ and the band energies $\epsilon_{k,\lambda}$ and by the self-consistent electronic charge density, respectively. Restricting equation (2.7) to the valence electrons we included also the core electrons in $K_{s,c}$ by transforming their contribution to the so-called core polarization term (Cohen *et al* 1959, Ebert *et al* 1986). The function χ_q^s in its full dependence on the spatial coordinates has thereby been employed for polarizing the core electrons together with the external field. We thus write $K_{s,c} = K_{s,cval} + K_{cp}$. We calculated $K_{\mathrm{orb,para}}$ by generalizing the formula for χ_q^{mom} derived by Götz and Winter (1989) to the case of many atoms per unit cell. It is given by the following relation:

$$\chi_q^{mom\,\alpha\beta}(\rho\kappa, \rho'\kappa'; 0) = -\frac{2}{\pi} \int \frac{\mathrm{d}k}{\Omega_{BZ}} \int \mathrm{d}\epsilon \, f(\epsilon) \lim_{\rho_1 \to \rho} \left\{ \lim_{\rho_1' \to \rho'} \left[\left(\frac{\partial}{\partial \rho_\alpha} - \frac{\partial}{\partial \rho_{1\alpha}} \right) \times \left(\frac{\partial}{\partial \rho'_\beta} - \frac{\partial}{\partial \rho'_{1\beta}} \right) \mathrm{Im}[g_k(\rho\kappa, \rho'\kappa'; \epsilon) g_{k+q}(\rho_1'\kappa', \rho_1\kappa; \epsilon] \right] \right\}. \tag{2.8}$$

Here, $f(\epsilon)$ is the Fermi distribution function and the k-integral is over the volume Ω_{BZ} of the Brillouin zone (BZ).

In conclusion we emphasize that to calculate K it is essential to know the full space dependence of the correlation functions χ_q and we exemplify this by writing $K_{s,cval}$ (2.6) in a more explicit form replacing for merely illustrational purposes χ^s with χ^{sP}. Representing the states $\psi_{k,\lambda}$ by the expressions

$$\psi_{k,\lambda}(\rho\kappa) = \sum_{l,m} c_{k\lambda,lm}^{\kappa} Y_{lm}(\hat{\rho}) R_l(\rho\kappa; \epsilon_{k\lambda})$$

where $Y_{lm} R_l$ is the single-site wavefunction with angular momentum quantum numbers l and m and where the c are the Bloch state coefficients, we obtain

$$\sum_{\kappa'} \int \mathrm{d}\rho' \, I_{\alpha\kappa} \chi_q^{sP\,\alpha\alpha}(0\kappa, \rho'\kappa'; 0) = \lim_{q,\omega \to 0} \left(\sum_{\kappa'} I_{\alpha\kappa} \frac{1}{4\pi} \times \sum_{\substack{\lambda,\lambda' \\ l_3 m_3}} \int \frac{\mathrm{d}k}{\Omega_{BZ}} \frac{f(\epsilon_{k+q\lambda}) - f(\epsilon_{k\lambda'})}{\epsilon_{k+q\lambda} - \epsilon_{k\lambda'} + \omega + \mathrm{i}\eta} \times c_{k+q\lambda,00}^{\kappa} c_{k\lambda',00}^{*\kappa} c_{k+q\lambda,l_3m_3}^{*\kappa'} c_{k\lambda',l_3m_3}^{\kappa'} R_0(0\kappa, \epsilon_{k+q\lambda}) R_0(0\kappa, \epsilon_{k\lambda'}) \right). \tag{2.9}$$

So for this quantity only the $l = 0$ components of the state vectors play a role at the site κ. The static homogeneous susceptibility χ^{sP}, on the other hand, i.e. the diagonal part of the double Fourier transform of χ^{sP}, is given by

$$\sum_{\kappa'} \chi^{sP}_{\kappa\kappa'} = \lim_{q,\omega\to 0} \left(\sum_{\substack{\lambda,\lambda' \\ l_1 m_1, l_2 m_2}} \int \frac{dk}{\Omega_{BZ}} \frac{f(\epsilon_{k+q\lambda}) - f(\epsilon_{k\lambda'})}{\epsilon_{k+q\lambda} - \epsilon_{k\lambda'} + \omega + i\eta} \times c^{\kappa}_{k+q\lambda, l_1 m_1} c^{*\kappa}_{k\lambda', l_1 m_1} c^{*\kappa'}_{k+q\lambda, l_2 m_2} c^{\kappa'}_{k\lambda', l_2 m_2} \right). \tag{2.10}$$

According to (2.10) all angular momentum components of the state vectors enter χ^{sP} and no simple relation between χ^{sP} and $K_{s,cval}$ exists. Analogous considerations hold for the interacting quantities. Likewise, no general relation exists between $K_{orb,para}$ and χ^{orb}, as can be seen by comparing equation (2.6) with the relations determining χ^{orb} (Götz and Winter 1989).

3. The LSDFA band structure

LMTO ASA calculations for the tetragonal structure, analogous to those performed by Temmerman *et al* (1987), provided the electronic data for constructing the one-particle Green function of the electrons. Fifty bands above the Y 4p, the Ba 5s and 5p, and the O 2s semicore states have been taken into account to calculate the imaginary parts of the correlation functions and to gain their real part by then applying the Kramers–Kronig relation. The band energies and the state vectors have thereby been evaluated on a tetrahedral mesh of 1125 k-points in the irreducible wedge of the BZ. Two significantly planar Cu (Cu2)–planar O (O2, O3) hybridized bands and one mainly chain Cu (Cu1)-dominated band cross the Fermi level ϵ_F, giving rise to a relatively low value of 44.4 states Ryd^{-1}/unit cell for the DOS at ϵ_F. The 5 eV broad high DOS complex below ϵ_F is an admixture of contributions from all atoms, including the apex O (O1), the chain O (O4), the Y and the Ba atoms. This is visualized by the partial DOS displayed in figure 1. The features beyond the 0.7 eV broad gap above ϵ_F are almost entirely due to the Y and Ba atoms. The considerable hybridization of the characters of the state coefficients is paralleled by their rapid change as k moves through the BZ. We illustrate this by displaying the characters of some typical bands at the Γ point and the X (0.5, 0, 0 d.u.) point and also showing their BZ-averaged characters in table 1. These features lead to the expectation that the amplitudes of the interband electron–hole transitions are severely reduced by matrix element effects. A further cause for their depression is the difference between the character of the states below and above ϵ_F. It is also important to note in this connection the weak dispersion of the bands in z direction.

4. Results for the Knight shift

Our theoretical data, obtained by evaluating equations (2.6) are displayed in tables 2–6. The individual contributions to K for the different atoms in the unit cell are listed. Most striking are the magnitude and the anisotropy of $K_{orb,para}$ (table 2)

Table 1. The leading contributions to the state vectors (in per cent) of the bands in the vicinity of the Fermi energy at the Γ and the X point and averaged over the BZ and the eigenvalues (in Rydbergs) at the Γ and the X point relative to ϵ_F (LMTO results).

Band	$\epsilon(\Gamma)$	Γ	$\epsilon(X)$	X	$\langle\Omega_{BZ}\rangle$
25	−0.1183	Cu2 d 51 O3 p 27 O2 p 11	−0.1293	Cu2 d 47 Cu1 d 31 O3 p 10	Cu2 d 49 Cu1 d 11 O3 p 8
26	−0.1177	Cu2 d 51 O2 p 26 O3 p 11	−0.1248	Cu1 d 62 O1 p 22 Ba d 5	Cu2 d 52 O2 p 10 Cu1 d 10
27	−0.1004	O2 p 38 O3 p 24 Cu2 d 18	−0.1062	Cu2 d 66 O1 p 13 O3 p 11	Cu2 d 59 O3 p 10 O2 p 10
28	−0.0974	O3 p 36 O2 p 22 Cu2 d 17	−0.1019	Cu2 d 78 O2 p 15 Y s 3	Cu2 d 54 O3 p 10 O2 p 9
29	−0.0925	Cu2 d 86 O2 p 4 O3 p 4	−0.0992	Cu2 d 48 Cu1 d 20 O1 p 17	Cu2 d 47 Cu1 d 11 O1 p 9
30	−0.0824	Cu2 d 74 O2 p 14 O1 p 4	−0.0936	Cu2 d 74 O2 p 18 Y d 7	Cu2 d 45 Cu1 d 12 O1 p 10
31	−0.0583	Cu2 d 39 O3 p 19 O4 p 19	−0.0731	Cu2 d 54 O2 p 34 O3 p 4	Cu2 d 39 O1 p 12 Cu1 d 11
32	−0.0511	Cu1 d 49 O1 p 14 Cu2 d 12	−0.0727	Cu2 d 58 O1 p 16 O3 p 13	Cu2 d 27 O4 p 19 Cu1 d 17
33	−0.0378	O1 p 66 Ba f 13 O4 p 10	−0.0714	Cu2 d 56 O2 p 32 Y f 7	Cu2 d 25 O4 p 20 O1 p 16
34	−0.0252	O1 p 60 Cu1 d 22 Ba f 11	−0.0454	Cu2 d 50 Cu1 d 20 O1 p 6	Cu2 d 42 Cu1 d 13 O3 p 11
35	−0.0239	O1 p 60 Cu1 d 21 Ba f 12	−0.0145	Cu2 d 34 Cu1 d 22 O1 p 12	Cu2 d 46 O3 p 14 O2 p 12
36	−0.0239	O1 p 49 O4 p 22 Ba f 17	−0.0020	Cu2 d 65 O2 p 17 Cu2 s 8	Cu1 d 29 Cu2 d 22 O1 p 14

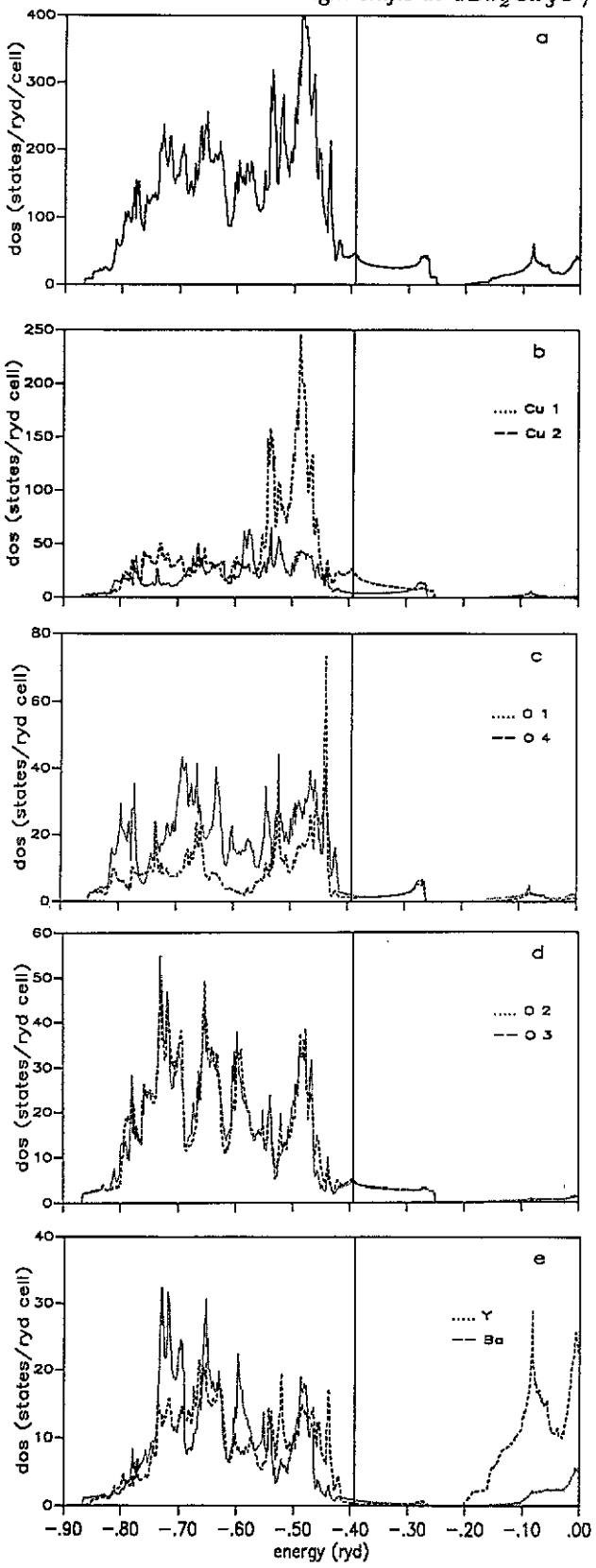

Figure 1. The densities of states of the LMTO band-structure of $YBa_2Cu_3O_7$ (the vertical lines at $\epsilon = -0.393$ Ryd designate the Fermi energy): (a) total DOS; (b) partial DOS at the Cu sites; (c) partial DOS at the chain-related (O4) and the apex (O1) oxygen atoms; (d) partial DOS at the planar oxygen atoms; (e) partial DOS at the Y and the Ba atoms.

Table 2. Paramagnetic orbital contributions to the Knight shifts of the individual atoms for the different directions of the magnetic field.

Atom	$K_{\mathrm{orb,para}}(\boldsymbol{H}\|\|a)$	$K_{\mathrm{orb,para}}(\boldsymbol{H}\|\|b)$	$K_{\mathrm{orb,para}}(\boldsymbol{H}\|\|c)$
Cu2	0.2155	0.2294	1.3449
O3	0.0054	0.0152	−0.0086
O2	0.0143	0.0084	−0.0054
O1	0.0053	0.0138	0.0483
Cu1	0.5861	0.1591	0.2877
O4	0.0116	0.0303	0.0315
Y	0.0067	0.0100	0.0185
Ba	0.0107	0.0119	0.0274

at the Cu sites. For the planar Cu atom the difference is a factor of more than 5 depending on whether the orientation of $\boldsymbol{H}$ is parallel or perpendicular to the x–y plane. The non-existence of fourfold symmetry is manifested in the slight difference between the values for $K^{\mathrm{Cu2},x}_{\mathrm{orb,para}}$ and $K^{\mathrm{Cu2},y}_{\mathrm{orb,para}}$. The corresponding data for the chain Cu atom are markedly different and it is not surprising that they depend greatly on whether $\boldsymbol{H}$ points in the x direction (perpendicular to the Cu–O chains) or in the y direction (parallel to the Cu–O chains). The values at the other sites are comparatively insignificant.

Appreciable contributions to $K_{\mathrm{orb,dia}}$ (table 3) are due only to the Cu, Y and Ba core electrons. However, these do not enter the experimental Knight shift, since the latter is measured relative to diamagnetic compounds containing the atom in question and $K_{\mathrm{orb,diacore}}$ is assumed to be equal in both systems. The valence electron contribution to $K_{\mathrm{orb,dia}}$ on the other hand is almost negligible.

Among the spin terms, the Fermi-contact term $K_{\mathrm{s,c}}$ is isotropic in the approximations of our treatment (table 4, second column). There is a marked difference between the values for the Cu1 and the Cu2 sites. The experimentally deduced anisotropy of K_{spin} is—at the level of our treatment—due to the term $K_{\mathrm{s,dip}}$ (table 5). In the case of cubic symmetry, $K^{(1)}_{\mathrm{s,dip}}$ would be exactly cancelled by $K^{(2)}_{\mathrm{s,dip}}$. In the present case of a tetragonal structure this cancellation is rather imperfect, especially at the Cu sites. At the Cu2 atoms, $K_{\mathrm{s,dip}}$ turns out to be positive for $\boldsymbol{H}$ in the x–y plane whereas for $\boldsymbol{H}$ parallel to the c axis we obtain negative values. At the Cu1 atoms, $K_{\mathrm{s,dip}}$ is considerably smaller. The core polarization contributions K_{cp}, decomposed in table 6 with respect to the values provided by the different core s shells counteract $K_{\mathrm{s,c}}$, but their relative magnitudes are smaller than found previously (Ebert *et al* 1986) for the case of some elemental transition metals, where they tend almost to compensate $K_{\mathrm{s,c}}$. The values for the total Knight shifts at the different atoms which depend on the direction of the magnetic field $\boldsymbol{H}$ are listed in table 4 (third to fifth columns).

5. Comparison with experiment

The NMR experiments of different groups have been compiled and analysed by Walstedt and Warren (1990). These workers have collected the data into a systematic order by working out a phenomenological model related to the work of Mila (1988) and Mila and Rice (1989a, b). The curves for the Knight shift due to Pennington *et*

Table 3. Diamagnetic contributions to the Knight shifts.

Atom	Core	Core+semicore	Valence	Total
Cu2	−0.2188	−0.2190	−0.0244	−0.2434
O3	−0.0270	−0.0315	−0.0075	−0.0390
O2	−0.0270	−0.0315	−0.0075	−0.0390
O1	−0.0270	−0.0315	−0.0082	−0.0397
Cu1	−0.2188	−0.2190	−0.0245	−0.2435
O4	−0.0270	−0.0315	−0.0082	−0.0397
Y	−0.3597	−0.3698	−0.0028	−0.3726
Ba	−0.6160	−0.6264	−0.0011	−0.6274

Table 4. Fermi contact contribution to the Knight shifts (second column) and the total values of K (third to fifth columns).

Atom	$K_{s,c}$	$K(H\|\|a)$	$K(H\|\|b)$	$K(H\|\|c)$
Cu2	0.4454	0.6680	0.6395	1.4531
O3	0.0279	0.0095	0.0604	0.0001
O2	0.0250	0.0587	0.0083	−0.0025
O1	0.0023	−0.0086	0.0024	0.0534
Cu1	0.2684	0.7143	0.4114	0.5567
O4	0.0266	0.0228	0.0609	0.0431
Y	0.0050	0.0081	0.0107	0.0165
Ba	0.0114	0.0199	0.0211	0.0372

al (1988) and to Barrett *et al* (1990) referring to the stoichiometric compound show a strong anisotropy with respect to the direction of the magnetic field. $K^{Cu2,x(y)}$, for example, is a factor of more than 2 smaller than $K^{Cu2,z}$. As the curves for both $K_{\|z}$ and $K_{\perp z}$ above the superconducting transition temperature T_c are rather temperature independent, extrapolation to $T = 0$ and thus comparison with our results is easily possible. Moreover, since $K_{\|z}$ shows hardly any change at and below T_c, whereas $K_{\perp z}$ drops sharply, it is generally concluded that K_{spin}, which should be strongly suppressed by the s-wave pairing mechanism in the superconducting state, contributes significantly to $K_{\perp z}$, but not to $K_{\|z}$. Our results are in reasonable agreement with these observations. We obtain for the planar Cu atoms the total values $K_{\|z} = 1.45\%$, $K_{\|x} = 0.67\%$ and $K_{\|y} = 0.65\%$, the latter lying somewhat above the experimental results of Takigawa *et al* (1989b) ($K_{\|z} = 1.27\%$ and $K_{\perp z} = 0.607\%$). Because of the anisotropic nature of the spin-dipole term adding to the Fermi-contact and the core polarization contribution, K_{spin} for Cu2 shows a large amount of the experimentally suggested anisotropy ($K_{spin}^{Cu2,z} = 0.129\%$, $K_{spin}^{Cu2,x} = 0.482\%$ and $K_{spin}^{Cu2,y} = 0.45\%$), although $K_{spin}^{Cu2,z}$ is not exactly zero. Most pronounced, however, and in accordance with experiment is the pronounced anisotropy of K_{orb}^{Cu2}.

For the Knight shifts at the chain Cu atom we obtain the total values $K^{Cu1,z} = 0.56\%$, $K^{Cu1,x} = 0.715\%$ and $K^{Cu1,y} = 0.411\%$. If we contrast these numbers to the corresponding experimental results (Takigawa *et al* 1989b), which are 0.60%, 1.338% and 0.607%, respectively, we find reasonable agreement for $K^{Cu1,z}$ but considerable deviations for the other two values. The principal causes for these differences are the orbital parts $K_{orb,para}$ of K. Takigawa *et al* (1989b), as well as

Table 5. Spin-dipole contributions to the Knight shifts. The first and the second columns for each magnetic field direction refer to the first and the second terms, respectively, of $K_{s,dip}$ *in equation* (2.6).

	$H\|\|a$			$H\|\|b$			$H\|\|c$		
Atom	$K^1_{s,dip}$	$K^2_{s,dip}$	$K_{s,dip}$	$K^1_{s,dip}$	$K^2_{s,dip}$	$K_{s,dip}$	$K^1_{s,dip}$	$K^2_{s,dip}$	$K_{s,dip}$
Cu2	−0.538 52	0.667 44	0.128 92	−0.538 52	0.625 06	0.086 54	−0.538 52	0.323 12	−0.215 40
O3	−0.043 85	0.028 62	−0.015 23	−0.043 85	0.069 78	0.025 93	−0.043 85	0.033 17	−0.010 68
O2	−0.044 92	0.073 62	0.028 70	−0.044 92	0.029 07	−0.015 85	−0.044 92	0.032 06	−0.012 86
O1	−0.019 33	0.012 17	−0.007 16	−0.019 33	0.014 67	−0.004 66	−0.019 33	0.031 17	0.011 84
Cu1	−0.164 06	0.075 70	−0.088 36	−0.164 06	0.199 94	0.035 88	−0.164 06	0.216 57	0.052 51
O4	−0.020 97	0.014 34	−0.006 63	−0.020 97	0.033 77	0.012 80	−0.020 97	0.014 81	−0.006 16
Y	−0.007 68	0.009 02	0.001 34	−0.007 68	0.008 41	0.000 73	−0.007 68	0.005 63	−0.002 05
Ba	−0.002 76	0.002 58	−0.000 18	−0.002 76	0.002 55	−0.000 21	−0.002 76	0.003 15	0.000 39

Table 6. The core polarization contributions to the Knight shifts. The values due to the individual core s shells are also shown.

Atom	1s	2s	3s	4s	5s	Total
Cu2	−0.011 81	−0.229 32	0.143 74			−0.097 39
O3	−0.014 22	0.013 19				−0.001 03
O2	−0.015 26	0.013 53				−0.001 73
O1	−0.006 63	0.005 69				−0.000 94
Cu1	−0.003 09	−0.067 78	0.043 43			−0.027 44
O4	−0.006 72	0.006 07				−0.000 65
Y	−0.000 20	−0.000 11	−0.000 04	−0.001 88		−0.002 23
Ba	−0.000 03	−0.000 03	−0.000 19	−0.000 04	−0.000 63	−0.000 92

other workers, obtain an approximate decomposition of K into its orbital and its spin part by assuming that K_{orb} is temperature independent, whilst K_{spin} vanishes in the superconducting state at zero temperature. They deduce the values $K^{Cu1,x}_{orb} = 1.18\%$ and $K^{Cu1,y}_{orb} = 0.43\%$. We find that $K^{Cu1,x}_{orb} = 0.562\%$ and $K^{Cu1,y}_{orb} = 0.135\%$. So, our results show considerable anisotropy—in agreement with experiment—but their magnitudes, however, are substantially smaller. For $H\|z$, our individual results for K_{orb} and K_{spin} are also reasonably near to experimental values. The same is true for all magnetic field directions in the case of the planar Cu atom.

6. Comparison of the present treatment with models

Pennington *et al* (1988), Mila and Rice (1989a, b) and also Walstedt and Warren (1990) analyse the Knight shift (and the spin–lattice relaxation) data on the basis of a phenomenological hyperfine Hamiltonian and a tight-binding Hubbard model for the electronic structure. The parameters of the latter have been derived by Mila (1988) who fitted his Hamiltonian to the band-structure results of Matheiss (1987), the photoemission data of Shen *et al* (1987) and the optical measurements of Etemad *et al* (1988) and Geserich *et al* (1988). Mila and Rice were forced to augment the simplest possible hyperfine Hamiltonian with an isotropic contribution. Their

Table 7. The ten band combinations yielding the leading contributions to the paramagnetic orbital Knight shifts.

$H\|\|a$		$H\|\|b$		$H\|\|c$	
$\lambda\lambda'$	$K^{\lambda\lambda'}_{\text{orb,para}}$	$\lambda\lambda'$	$K^{\lambda\lambda'}_{\text{orb,para}}$	$\lambda\lambda'$	$K^{\lambda\lambda'}_{\text{orb,para}}$
35 34	0.017 62	36 27	0.012 79	35 28	0.173 42
35 25	0.011 12	36 35	0.011 97	34 27	0.098 07
34 33	0.010 75	36 26	0.009 61	34 29	0.076 65
35 29	0.009 59	35 30	0.007 79	36 30	0.072 61
35 27	0.008 78	35 34	0.007 49	35 27	0.062 20
34 28	0.007 45	34 31	0.006 57	35 30	0.059 77
35 26	0.007 42	35 25	0.006 16	35 31	0.058 13
34 26	0.007 15	36 29	0.005 92	35 29	0.055 72
34 30	0.007 14	35 27	0.005 85	34 26	0.046 41
35 30	0.006 85	35 32	0.005 44	34 25	0.045 77

Hamiltonian for the planar Cu atom is

$$H_{\text{hf}}^{\text{Cu2}} = \sum_j A^\alpha I_{j\alpha} S_{j\alpha} + \sum_i B\sigma_i \cdot I. \tag{6.1}$$

Here, the sums are over the Cu2 sites. The first term in equation (6.1) is attributed to the on-site nuclear spin–electron spin interaction, whereas the second is interpreted as a hyperfine interaction, transferred from the neighbouring Cu spin. K_{orb} is analysed by Mila and Rice as follows. They write it as the product of the static homogeneous orbital susceptibility χ_{orb} and the orbital part A_{orb} of the tensor **A**, whereby A_{orb} is assumed to be proportional to some spatial average of $1/r^3$ with r the electron coordinate relative to the nucleus. Whilst the values for K_{orb} and χ_{orb} are taken from the experiments of Takigawa *et al* (1989b), A_{orb} is obtained from EPR data for the Cu^{2+} ion. A similar *ansatz* is made for K_{spin}. This quantity is written as the product of the spin susceptibility χ_{spin} and the spin part A_{spin}, of the phenomenological tensor **A**. Again, taking the values for K_{spin} and χ_{spin} from the work of Takigawa *et al* (1889b), Mila and Rice evaluate A_{spin}. Connecting A_{spin} with the probability density of the electronic ground-state wavefunction at the origin, Mila and Rice find reasonable parameters describing the admixture of the different atomic wavefunctions in the assumed tight-binding ground-state wavefunction. To interpret the van Vleck part of χ_{orb} and K_{orb}, these workers assume that transitions mainly between $d_{x^2-y^2}$ and d_{xy} orbitals at the planar Cu site and transitions between $d_{x^2-y^2}$ and d_{xy} as well as d_{yz} orbitals at the chain Cu atoms determine these quantities. From the experimental values for χ_{orb} they derive the excitation energies of those local orbitals.

In contrast, our *ab-initio* LSDFA band-structure-based calculations use no fitting parameters but yield directly the experimentally determined quantities. The various contributions to K are not written as the product of susceptibilities at q equal to zero and some average of $1/r^3$ or the probability density of some wavefunction at the nucleus, respectively. As discussed in section 2, such decompositions are not exactly valid. Indeed, in their treatment of elemental transition metals, Ebert *et al* (1986) show that the product of χ_{orb} and the expectation value of $1/r^3$ formed using the prescription of Clogston *et al* (1964) leads to values markedly different from the results obtained by applying equation (2.6). Likewise, applying the procedure of Mila

and Rice to K_{spin} proved problematic in the case of some transition metals, e.g. Pd (Stenzel and Winter 1988).

Whereas the contributions to K_{spin} (as well as to χ_{spin}) in the long-wavelength limit needed here come from intraband transitions within bands 34–36 in the neighbourhood of ϵ_F, the contributions to K_{orb} are due to transitions between all occupied bands in the high-DOS complex below ϵ_F and the unoccupied parts of bands 34–36. As an illustration we give the ten band combinations providing the leading contributions to K_{orb} in table 7. It is obvious that these combinations depend strongly on the direction of $\boldsymbol{H}$ and that the sum is considerably smaller than K_{orb}, emphasizing the importance of other bands as well. The characters of these bands, shown in table 1, demonstrate that we are dealing here with transitions between partly Cu d-like bands which, however, show strong hybridization effects with other atoms.

One should keep in mind that K_{orb} and χ_{orb} (which are much stronger than K_{spin} and χ_{spin}) depend on details of the characters of the state coefficients, since the matrix elements entering the latter quantities are dominated by the scattering between states with strong Cu d and O p characters of different symmetries. So the results for K_{orb} are very sensitive to the hybridization of Cu d and O p and therefore it is worthwhile to repeat the present calculations using band-structure methods different from the LMTO ASA. This is at present being done on the basis of the more rigorous KKR method and for comparison with table 1 we present the characters of some bands at the Γ and the X points as well as BZ-averaged values resulting from KKR band-structure work in table 8. Whether the KKR-based calculations lead to improved results for $K^{Cu1,x}_{orb,para}$ and $K^{Cu1,y}_{orb,para}$ remains to be seen.

Finally, we come to the conclusion that a closer relationship between our treatment and the tight-binding Hubbard model analysis of the above-mentioned workers is hard to establish.

7. Conclusions

Our LSDFA RPA band-structure-based *ab-initio* treatment of the zero-temperature Knight shifts in the high-T_c superconducting compound $YBa_2Cu_3O_7$ yields encouraging results. Except for $K^{Cu1,x(y)}_{orb,para}$, our theoretical data for the Cu atoms are as near to experiment as one can expect for this kind of approximation at all. The relative deviations are not large, as found in the case of other systems for which it is agreed that the band-structure approach performs well: elemental transition metals (Ebert *et al* 1986) and simple metals (Götz and Winter 1991). Besides $K^{Cu1,x(y)}_{orb,para}$, the magnitudes of the corresponding quantities at the Y and the O sites—apart from being small—also do not agree overly well with the experimental values of Alloul *et al* (1989) and Takigawa *et al* (1989a). However, as they depend sensitively on details of the state vectors, differences have not necessarily to be counted as serious drawbacks of the LSDFA band-structure method. It is quite possible that the application of a more rigorous method will diminish these remaining unsatisfactory features of our theoretical results. Investigations on this point using the KKR are currently under way. It is also planned in the near future to compute the spin–lattice relaxation times as well as the wavevector-dependent dynamical spin susceptibility. As the wavevectors q in the whole BZ with special emphasis on the BZ boundary enter these quantities, calculations of this kind are a still more stringent test for the

Table 8. The leading contributions to the state vectors (in percent) of the bands in the vicinity of the Fermi energy at the Γ and the X point and averaged over the BZ and the eigenvalues (in Rydbergs) at the Γ and the X point relative to ϵ_F (KKR results).

Band	$\epsilon(\Gamma)$	Γ	$\epsilon(X)$	X	$\langle\Omega_{BZ}\rangle$
25	−0.1560	O1 p 20 O2 p 20 O4 p 18	−0.1553	Cu2 d 56 Cu1 d 26 O3 p 9	Cu2 d 51 Cu1 d 13 O4 p 9
26	−0.1509	Cu2 d 30 O3 p 25 Cu1 d 16	−0.1405	Cu1 d 58 O1 p 24 Ba d 8	Cu2 d 44 Cu1 d 21 O1 p 10
27	−0.1505	Cu2 d 31 O2 p 24 Cu1 d 16	−0.1263	Cu2 d 44 O1 p 21 O4 p 18	Cu2 d 49 Cu1 d 15 O1 p 10
28	−0.1502	Cu2 d 66 Cu1 d 21 O3 p 4	−0.1232	Cu2 d 80 O2 p 14 Y d 2	Cu2 d 53 Cu1 d 14 O3 p 8
29	−0.1249	Cu2 d 42 O2 p 23 O3 p 16	−0.1185	Cu2 d 33 Cu1 d 30 O1 p 22	Cu2 d 50 Cu1 d 14 O1 p 8
30	−0.1135	O1 p 29 Cu2 d 28 O3 p 14	−0.1105	Cu2 d 74 O2 p 21 Y d 4	Cu2 d 44 Cu1 d 16 O1 p 10
31	−0.1058	Cu2 d 89 O2 p 3 O3 p 3	−0.0976	Cu2 d 62 O2 p 33 O3 p 1	Cu2 d 40 Cu1 d 18 O1 p 12
32	−0.1013	O1 p 36 Cu1 d 28 Cu2 d 15	−0.0952	Cu2 d 63 O2 p 32 Y p 2	Cu2 d 43 Cu1 d 15 O1 p 12
33	−0.1011	O1 p 36 Cu1 d 29 Cu2 d 15	−0.0886	Cu2 d 58 O1 p 22 O3 p 9	Cu2 d 54 O1 p 15 O3 p 8
34	−0.0987	Cu2 d 79 O2 p 9 O3 p 5	−0.0557	Cu2 d 67 Cu1 d 9 O2 p 7	Cu2 d 54 O3 p 11 O2 p 10
35	−0.0866	Cu2 d 54 O1 p 21 O3 p 10	−0.0393	Cu1 d 42 O1 p 18 Cu2 d 17	Cu2 d 49 O3 p 15 O2 p 12
36	−0.0603	Cu1 d 49 O1 p 15 Cu2 d 11	−0.0137	Cu2 d 64 O2 p 20 Cu2 s 5	Cu1 d 28 Cu2 d 25 O1 p 12

validity of the band-structure description of this ceramic compound than the evaluation of the Knight shift is. Even if the theoretical results for these quantities turn out to be unsatisfactory, this would not be unavoidably a cause for abandoning the band-structure approach altogether in favour of some t–J- or Hubbard-model-based theories. It would then be worthwhile to apply improvements of the LSDFA, especially self-interaction corrections, which are already proving beneficial in some cases which seemed to be impracticable for LSDFA band-structure theory (Svane and Gunnarson 1988, Szotek *et al* 1991a, b) to $YBa_2Cu_3O_7$ as well.

References

Alloul H, Ohno T and Mendels P 1989 *Phys. Rev. Lett.* **63** 1700

Barrett S E, Durand D J, Pennington C H, Slichter C P, Friedmann T A, Rice J P and Ginsberg D M 1990 *Phys. Rev.* B **41** 6283

Bloembergen N and Rowland T J 1953 *Acta Metall.* **1** 731 (erratum 1955 *Acta Metall.* **3** 74)

Carter G C, Bannet L H and Kahan D J 1977 *Prog. Mater. Sci.* **20** 3–20

Clogston A M, Jaccarino V and Yafet Y 1964 *Phys. Rev.* A **134** 650

Cohen M H, Goodings D A and Heine V 1959 *Proc. Phys. Soc.* **73** 811

Cohen R E W, Pickett W E, Boyer L L and Krakauer H 1988 *Phys. Rev. Lett.* **60** 817

Ebert H, Winter H and Voitländer J 1986 *J. Phys. F: Met. Phys.* **16** 1133

Emergy V J 1991 *Physica* B **169** 17

Etemad S, Aspnes D E, Kelly M K, Thompson R, Tarascon J M and Hull G W 1988 *Phys. Rev.* B **37** 3396

Geserich H P, Scheiber G, Geerk J, Li H C, Linker G, Assmus W and Weber W 1988 *Europhys. Lett.* **6** 277

Götz W and Winter H 1989 *Solid State Commun.* **72** 739

—— 1991 *J. Phys.: Condens. Matter* **3** 8931

Hirch J E and Marsiglio F 1989 *Physica* C **162–4** 591

Leung T C, Wang X W and Harmon B N 1988 *Phys. Rev.* B **37** 384

Matheiss L F 1987 *Phys. Rev. Lett.* **58** 1028

Mila F 1988 *Phys. Rev.* B **38** 11 358

Mila F and Rice T M 1989a *Physica* C **157** 561

—— 1989b *Phys. Rev.* B **40** 11 382

Olsen C G, Liu R, Lynch D W, List R S, Arko A J, Veal B W, Chang Y C, Jiang P Z and Poulikas A P 1990 *Phys. Rev.* B **42** 38

Pennington C H, Durand D J, Zax D B, Slichter C P, Rice J P and Ginsberg D M 1988 *Phys. Rev.* B **37** 7944

Pickett W E 1989 *Rev. Mod. Phys.* **61** 433

Schwarz K, Ambrosch-Draxl C and Blaha P 1990 *Phys. Rev.* B **42** 2051

Shen Z, Allen J W, Yeh J J, Kang J S, Ellis W, Spicer W, Lindau I, Maple M P, Dalichaouch Y D, Torikachvili M S, Sun J Z and Geballe T H 1987 *Phys. Rev.* B **36** 8414

Stenzel E and Winter H 1985 *J. Phys. F: Met. Phys.* **15** 1571

—— 1986 *J. Phys. F: Met. Phys.* **16** 1789

—— 1988 unpublished

Stenzel E, Winter H, Szotek Z and Temmerman W M 1988 *Z. Phys.* B **70** 173

Svane A and Gunnarson O 1988 *Europhys. Lett.* **7** 171

Szotek Z, Temmerman W M and Winter H 1991a *Solid State Commun.* **74** 1031

—— 1991b *Physica* B **172** 19

Takigawa M, Hammel P C, Heffner R H, Fisk Z, Ott K C and Thompson J D 1989a *Physica* C **162–4** 853

Takigawa M, Hammel P C, Heffner R H, Fisk Z, Smith J L and Schwarz R 1989b *Phys. Rev.* B **39** 300

Temmerman W M, Szotek Z, Durham P J, Stocks G M and Sterne P A 1987 *J. Phys. F: Met. Phys.* **17** L319

Temmerman W M, Szotek Z and Guo G Y 1988 *J. Phys. C: Solid State Phys.* **21** L867

Walstedt R E and Warren W W 1990 *Science* **248** 1082

Winter H, Szotek Z and Temmerman W M 1990 *Z. Phys.* B **79** 241